Life Under the Ice:
The Effect of Ice Development on Photosynthetic Submerged Plants

BEE 4530: Computer-Aided Engineering

©Sochima Bishop, Rowan Callahan,

Luke Sendelbach

May 10, 2018

Table of Contents

Executive Summary

Many submerged plants rely on photosynthesis as a means to obtain sugars and oxygen. Plants that inhabit deeper regions have limited exposure to sunlight, as light irradiance decreases exponentially with increasing distance from the surface. During the winter, ice growth over a lake adds additional light obstruction. Ice sheets may grow to a thickness that reduces light availability to a level that no longer supports photosynthesis. While modeling the growth of ice sheets computationally is not new, there have not been studies linking ice sheet growth with the obstruction of light used for photosynthesis. This study investigates the conditions necessary to grow an ice sheet sufficiently thick to reduce the light irradiance 20 meter below the surface to 10% of the irradiance hitting the surface of the ice.

Our investigation looks at upstate New York and considers a region containing the expanding ice sheet, the water below it, and an insulating 2 centimeter thick layer of snow that only exists when an ice sheet does. To model the growth of the ice sheet we modelled the heat transfer and treated the ice layer as a solid with a no flow liquid water domain underneath. We included Syracuse specific time-dependent air temperature conditions, a convective heat transfer coefficient, radiative flux from sunlight and radiation from the atmosphere at the surface of the lake to mimic common wintertime conditions. We also used zenith angle information from upstate New York latitude and longitudes. A semi-infinite boundary at a constant temperature was established at the bottom of the domain to simulate a deep lake. Additionally, we incorporated water's temperature dependent density in modeling heat transfer in the domain. Finally, we implemented these design specifications (dimensions, equations, boundary conditions, and physics) in COMSOL software for numeric analysis for the duration of an entire month.

After implementing the model with the above conditions, we were able to show that our model successfully computes the growth and decay of ice over time for small northern lakes. We obtained a model of the temperature variation within the ice layer and water underneath at discrete points in time, as well as the depth of the ice sheet over the course of the time period. Our model demonstrated that ice formation never reached a thickness sufficient to impede photosynthesis in our Syracuse location given normal conditions and moderate future weather shifts. However, our model includes flexibility to incorporate a range of different weather conditions, which may be used to monitor whether climate change can drive ice formation enough to inhibit photosynthesis.

Keywords: Ice-formation, Photosynthesis, New York, COMSOL, heat transfer

Introduction

In many climates, the onset of winter is accompanied by lower temperatures, shorter days, and the accumulation of ice and snow. But what effect do these conditions, such as ice sheet formation on the surface of a lake, have on the life beneath? More specifically, does the ice layer impede photosynthesis?

Aquatic plants rely on photosynthesis as a means to obtain sugars and O_2 [1]. Ice growth over a lake can block sunlight necessary for photosynthesis, and some plants can experience over a 70% reduction in light-saturated net photosynthesis due to reduced light and cold, non-freezing water temperatures [2]. The irradiance of light that penetrates through water decreases exponentially as the distance from the surface increases, following the Beer-Lambert Law [3]. Plants can grow as deep as 70m with as little as 10% of the original surface irradiance, and this knowledge has allowed researchers to relate underwater light attenuation with depth limits [4]. Ice sheets formed over the surface of lakes act as an absorptive layer that light must pass through [1], decreasing light access to submerged plants. The amount of light that reaches a fixed point below the surface decreases as water freezes into ice because ice has a much higher absorption coefficient than water.

Over the course of the winter this ice sheet may grow to a thickness that would reduce light availability to a level where photosynthesis is no longer possible. A better, quantitative, understanding of the relationship between ice sheet growth and light inhibition is needed. Understanding this phenomenon is especially important in the age of climate change, where more and more extreme weather conditions can drastically alter local ecology.

Problem Statement

Currently, there exists computational knowledge about lake freezing [6] and about sunlight requirements for underwater plant life [1]. However, there was a lack of knowledge relating the two: how quantitatively the growth of ice sheets in the winter time limits the light available for photosynthesis below the ice sheet itself. Furthermore, ice sheet growth is obviously closely linked to weather, which in turn varies depending on where in the world you are. This means that location has strong link to the light that is available to underwater plants. So, an adaptable model that can receive many types of weather data would be a useful tool to generalize to any lake in the world. For our study, we chose to use Syracuse, NY as a starting point for generalization.

The goal of our study was to determine the duration (in days) until the surface of the water permanently freezes to a depth that inhibits photosynthesis under the ice, using Syracuse, NY as an example location.

Design Objectives

Our goal was to create a simple lightweight model that could incorporate local weather data and be used to create different predictions of ice depth variation given different weather conditions.

We modeled the lake as a one-dimensional heat conduction problem with time varying boundary conditions at the surface of the ice, which served as the top surface of the domain. This allowed us to examine sensitive local results because weather conditions are strongly dependent on the time of day and location.

The domain of the problem has constant dimensions, and includes the entire ice sheet, stagnant water underneath the sheet, and insulating snow above the sheet, which exists only when the ice sheet does. Time varying weather data was incorporated as an hourly interpolation function of the National Renewable Energy Lab's (abbreviated as NREL) typical meteorological year (abbreviated as TMY3) historical weather data for Syracuse, NY. This data is representative of what is considered typical in the locale we are interested in and was used as an adjustable baseline for sensitivity tests on a variant temperature distribution.

Additionally, we computed the depth of ice that is required to reduce the light penetration into the water to 10% of the surface irradiance, which is the threshold for the minimum irradiance that is sufficient for photosynthesis which we found to be 1.13 m. With this knowledge, we ran our model in COMSOL for the duration of a month, incorporating local weather conditions. We then extracted the position in the domain where the water temperature is equal to the freezing point. This location is the interface of the ice sheet and liquid water. Plotting this location over time allowed for the visualization of how the ice sheet grew and decayed. Finally, this allowed us to examine the point in time where the ice depth was equal to the depth that prohibits photosynthesis.

Methods

Overview

We modeled the freezing of a lake over the course of a month with weather and climatological conditions similar to those during a typical winter in upstate New York. Instead of modeling the growth of the ice sheet as a Stephan problem with a sharp, defined water ice interface, we expanded the interface into a small region where the water is partially frozen. We also added a thin, insulating layer of snow to the top of the domain that exists only when there is ice to support it. This layer of snow appears after the weather has gotten cold enough to form a layer of ice so as to prevent the unrealistic case where snow floats on top of water without sinking or melting. At the top of the snow layer we added a convective boundary condition as well as shortwave and longwave radiation from the sun.

As the water freezes into ice, it becomes more optically dense and is less permeable to light [2]. Therefore, as the liquid water freezes and the ice sheet grows, less light becomes available for photosynthesis.

Schematic

The geometry of the model and boundary conditions in words are shown in Figure 1. The domain is assumed to be pure water: solutes are not concentrated enough to see freezing point depression effects. Also important to note is that the computaional domain in COMSOL is only 6m deep and does not include the point 20m below the surface where we calculate light irradiance.

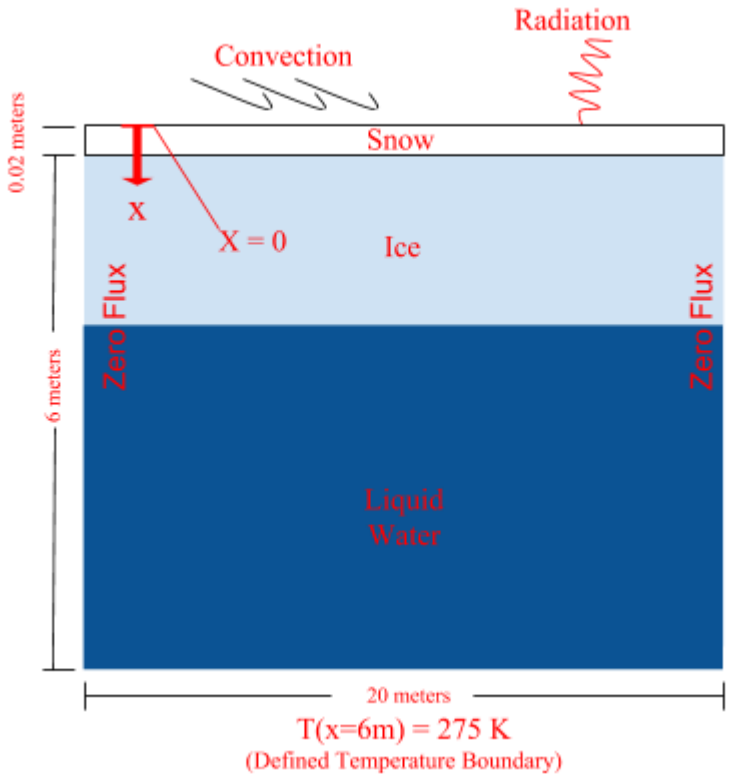

Fig. 1: Problem Schematic. The domain of the problem has constant dimensions, and includes the entire ice sheet along with zero flow water underneath the sheet. In this model, there is both time varying

convection and radiation contributing to heat transfer at the top boundary. The water is treated as semi-infinite where the bottom boundary 6m below the surface is held at a constant temperature of 275K.

In addition to standard heat conduction in the domain, heat transfer involved in the freezing process also needs to be considered. We modeled the freezing process as a graduated process where water freezes from between the temperatures of 273.05K and 273.25K (-0.1 ℃ and +0.1 ℃).

Governing Equations and Boundary Conditions

The relevant governing equation for this heat transfer problem includes a storage term and a conduction term; convection and radiation are only considered at the top boundary and are therefore not needed inside the domain. Equation 1 gives the governing equation for heat transfer within the domain, where T is absolute temperature, t is time, α is thermal diffusivity, and x is the position (depth) within the domain.

$$\frac{\partial T}{\partial x} = \alpha \frac{\partial^2 T}{\partial x^2} \tag{1}$$

The domain was modeled to include three regions: the bottom portion of the domain with a deep zero flow water layer that freezes from the top down, the ice that was once liquid, and the snow that receives solar and longwave radiation and is exposed to forced convection due to wind. Equation 2 describes the boundary condition at the top of the snow domain while equations 3 and 4 describe the net radiative solar flux term Q_S and the net longwave radiative flux Q_R, respectively. S represents the solar constant, Z represents the solar zenith angle, CN is the cloudiness factor, and vp is the water vapor pressure. Equation parameters are defined in Table 1 (Appendix A). The initial condition is simply that the entire domain has a temperature of 275K (2 °C) at t= 0.

$$Q_R + Q_S + h(T_{air} - T|_{x=0}) = -k \left.\frac{\partial T}{\partial x}\right|_{x=0} \tag{2}$$

$$Q_R = T_{air}^4 (0.746 + 0.066 \cdot \sqrt{vp})(1 + 0.26CN) - \varepsilon \sigma_s T|_{x=0}^4 \tag{3}$$

$$Q_S = \frac{S\cos^2 Z}{1.2\cos Z + (\cos Z + 1.0)vp \cdot 10^{-3} + 0.0455} \cdot (1 - 0.52CN) \tag{4}$$

Inside of the zero-flow water we modeled the freezing front over a small temperature range between 273.05K and 273.25K (-0.1 to 0.1℃). Inside this bound we increased the heat capacity of water such that the heat capacity (C_p) included the latent heat of fusion of water. This allowed us to easily track the freezing front of ice for calculating sheet depth. C_p values for water are displayed in Figure 2. These values were used to define a piecewise function where 334 kJ/kg is the latent heat of fusion to be spread over 273.05K and 273.25 (-0.1 to 0.1 °C) into the sensible heat capacity, and added to the average sensible heat capacity of liquid water and frozen ice. Varying snow depth and snow packing was ignored in favor of a static snow layer because the insulation value of snow-ice pack was found to be close enough to ice once it was packed down [8].

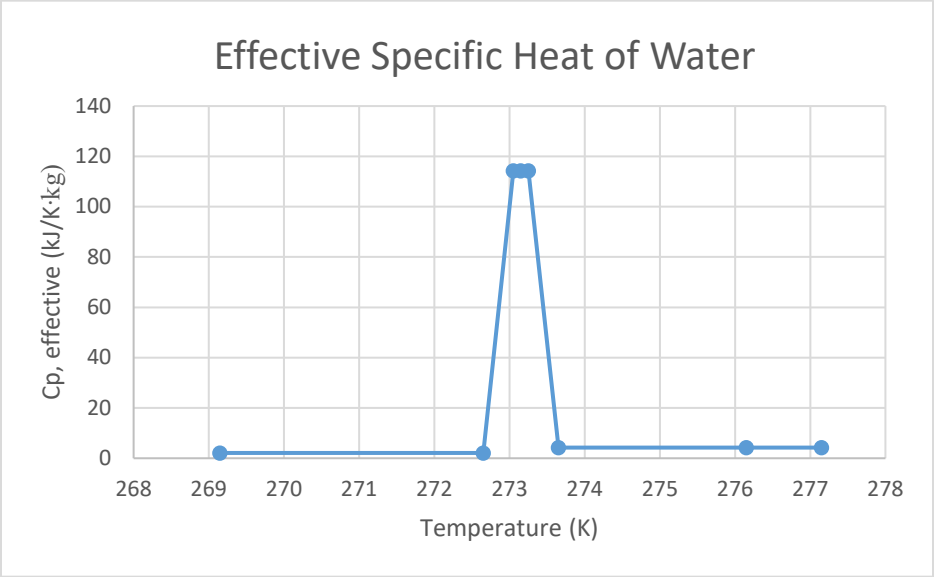

Fig. 2: Plot of effective specific heat values. This shows how the effective heat capacity varies with temperature to incorporate the latent heat of fusion. To the left of the peak, frozen ice is described. To the right of the peak, liquid water is described. The peak itself represents the partially frozen region.

At temperatures below freezing, the effective heat capacity of water is equal to that of sensible heat capacity of ice. Above freezing, the effective heat capacity of water is equal to that of the sensible heat capacity of liquid water. However, near the freezing point of water, the effective heat capacity is equal to the sum of the sensible heat capacity and the latent heat of fusion of water. Another parameter of interest is ρ, the mass density of water-ice. Figure 3 shows the temperature dependence of density used in our model.

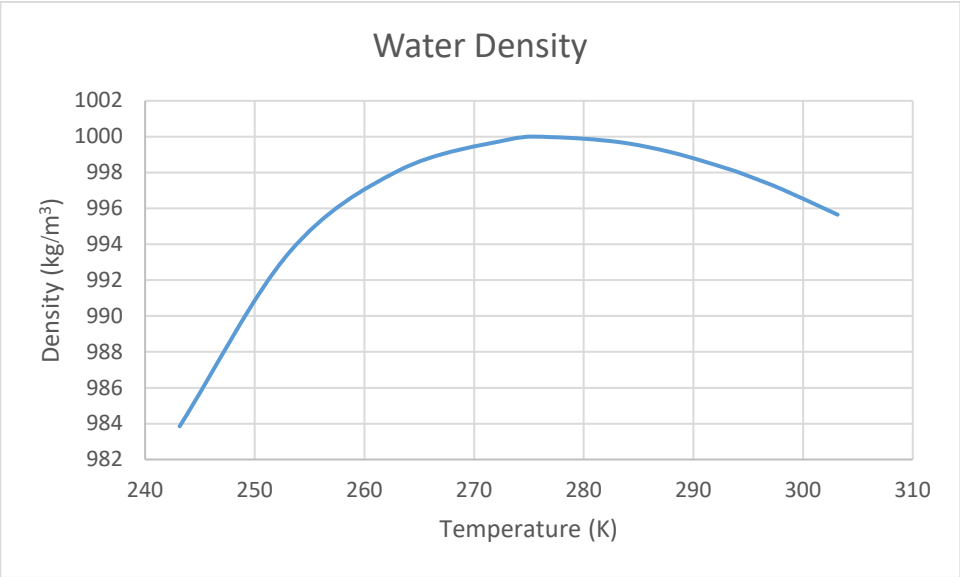

Fig. 3: Temperature dependence of density for water [7]. Water has is greatest density at 277 K. Water that is just below the ice is not only just above freezing, but is also less dense (and therefore floats on top of) the warmer water underneath it.

Notice that density peaks at 277 K (4 °C). This means that just below the bottom of the ice sheet (and just above the freezing point), water is at its least dense. This water that is just about to freeze into the ice sheet will float on top of the water column rather than sink down. This property of water limits natural convection, and is the basis of our zero bulk flow lake model, and creates the basis of our assumption that natural convection of the liquid water in the lake is negligible. This is why there is no convection term included in our governing equation.

We solved the Beer-Lambert equation in order to find the amount of light at any specific point below the surface. This equation was solved to a local solution presented below in equation 5, where α_{ice} is the spectrum absorption coefficient of pure bubble-free ice, α_{water} is the absorption coefficient of pure water, and x is the depth below the surface, and L is the amount of total light that gets through.

$$L = e^{(-a_{ice} \cdot x)} \cdot e^{(-\alpha_{water} \cdot 20\ m)} \tag{5}$$

Equation 6 was found by solving equation 5 to get the depth of ice needed to reduce irradiance at 20 meters below the surface to 10% of the light hitting the surface of the lake:

$$x = \frac{\ln(L) + \alpha_{water} \cdot 20m}{-\alpha_{ice}} \tag{6}$$

The solution to equation 6 was found and averaged over all wavelengths of light visible to plants. This averaged value was 1.13m of ice formation.

Model Implementation

The full model was implemented using 1D transient heat transfer through the semi-infinite domain. Air temperature and wind data was imported into COMSOL using typical meteorological historical data (TMY3) in Syracuse, NY for the month of January. These values are displayed below in Figure 4.

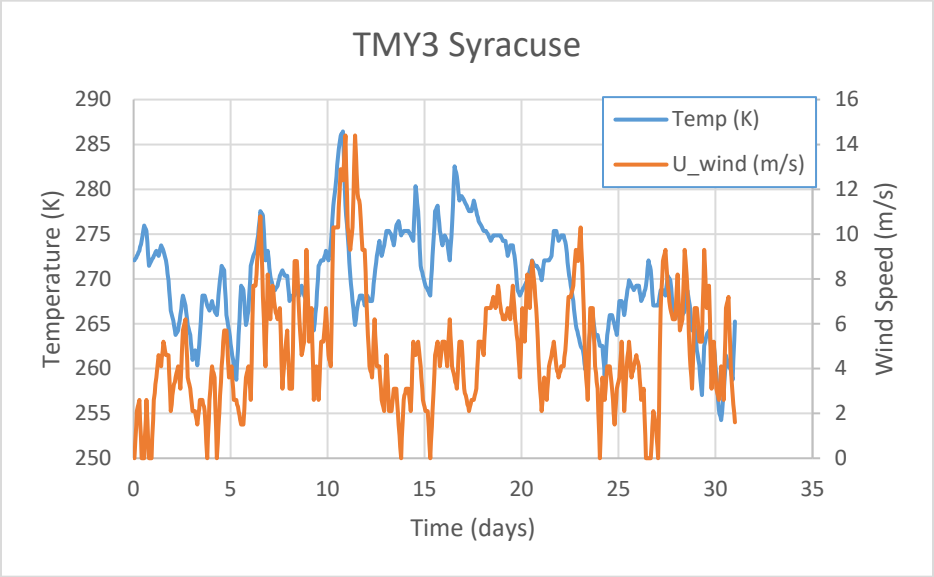

Fig. 4: TMY3 Syracuse. This is historical weather data for Syracuse, New York. It is taken from the NREL's published typical meteorological data, and is representative of a normal January in Syracuse [12].

The NREL creates the TMY3 by piecing together different months in history that are determined to be typical and normal for that particular location. For our study, we used the published historical data for a January in Syracuse, NY, which happens to be January of 1983. However, the COMSOL model can easily accommodate any weather data, not just from this particular place in this particular time period.

Solar radiative heat flux was incorporated as a function of these temperatures in a flux term defined in equation 3. This equation was coupled with a logic function to mimic the day night cycle where there is no solar radiation between 5:00pm 6:00am. Longwave radiative flux was incorporated as a function of zenith angle and cloudiness and is defined in equation 4. The heat transfer coefficient, h, was obtained analytically by considering the surface of the domain as a flat plate experiencing forced convection and manipulating the numerical relationship between the Nusselt (Nu), Reynolds (Re), and Prandtl (Pr) numbers.

$$h = Nu \cdot k/L \tag{7}$$

where L is the length of the plate and k is the thermal diffusivity.

$$Nu = 0.664 Re^{0.5} Pr^{0.33} \tag{8}$$

For laminar flow:

$$Re = U_m \cdot L/\nu \tag{9}$$

where L is the length of the plate, U_m is the fluid flow velocity (in this case wind speed) and ν = kinematic viscosity of air.

$$Pr = (\mu \cdot C_p)/k \tag{10}$$

Where μ is the dynamic viscosity of air.

Other parameters used in our model are defined below in Table 1. The problem was run for 30 days (720 hours).

Mesh Convergence

For our solution we chose a very fine mesh with a higher density of elements near the top of the domain, where the solution is changing the most. We chose to have the high element density near the top because spatial discretization error will be minimized in the most important area of the domain (where the ice sheet initially forms and grows). The mesh is displayed in Figure 5.

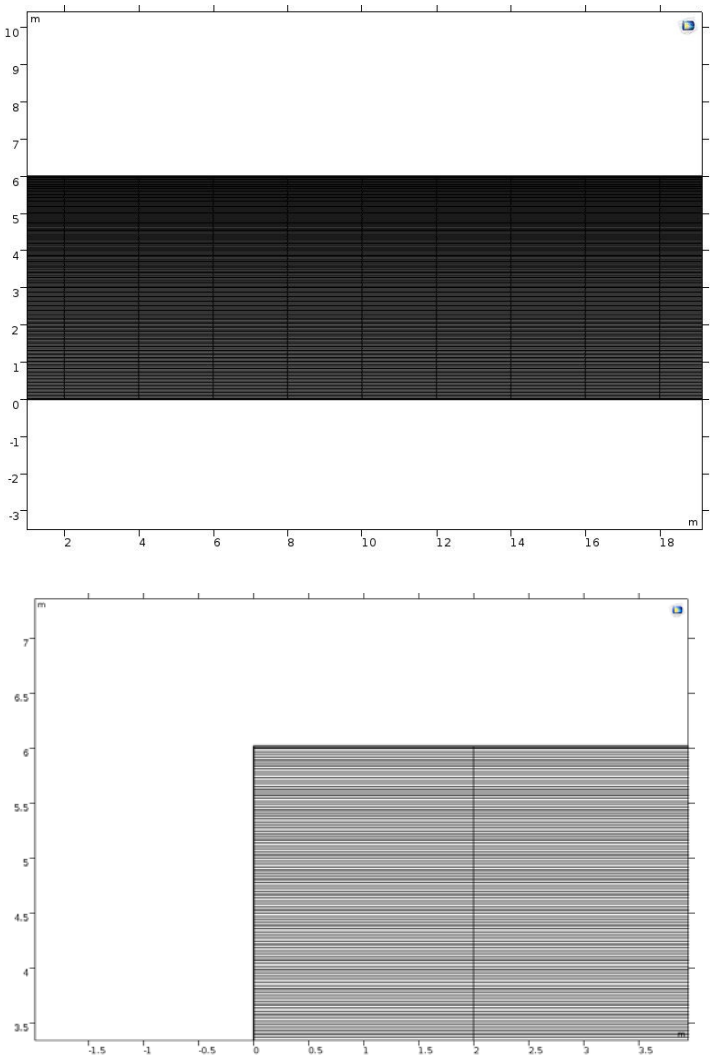

Fig 5: Mesh Schematic. The top image in the figure shows our mesh with 2000 elements in COMSOL. This is a cross section, where the y axis shows depth and the x axis runs horizontally. Each corner

represents a node, where COMSOL calculates the temperature and interpolates the solution in the spaces between the nodes. The bottom image in the figure shows a zoomed in section to show the trace of elements across the domain.

Notice that the top of the mesh in figure 15 is much darker than the bottom; this is indicative of the higher mesh density. We used a geometric sequence of 200 elements along the depth of the domain to achieve the varied size. The sequence was implemented in reverse order so that the top of the domain was denser than the bottom. To quantify the element growth rate along the depth, the growth rate was set to 1.3, meaning that an element is 1.3 times as large as the element just above it. In the horizontal direction, there is no heat flow, so 10 elements were linearly spaced along the length. In total, there are 2000 elements in our final mesh.

We used 2000 elements in order to minimize spatial discretization error without needlessly increasing computation time. We performed a mesh convergence (Figure 6) at a point 2 meters below the surface of the ice after 700 hours and found the solution to be relatively unchanged after 500 elements. We chose to use four times the observed minimum element number to ensure that the spatial discretization error is minimized.

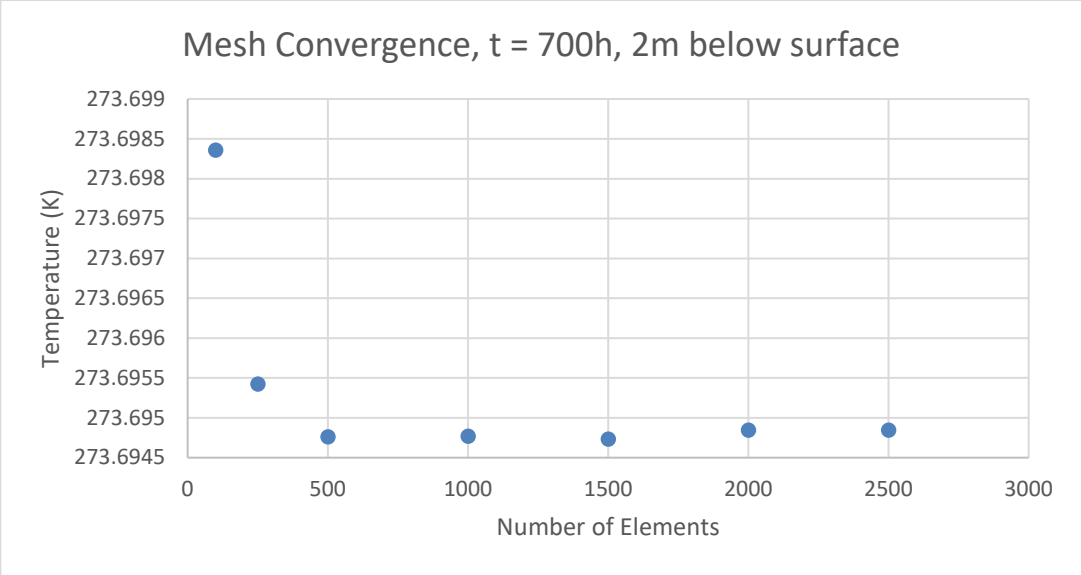

Fig. 6: Mesh Convergence. Mesh convergence is shown after 700 hours at a point 2 meters below the ice. Convergence suggests that computation running with 500 elements in the mesh is minimally sufficient to eliminate solution dependency on the mesh.

Worth noting is the tight range with which the mesh converges. Even changing from 100 elements to 250 elements changes the solution by only 1/1000 of a Kelvin. This degree of precision is much greater than what is actually needed to model ice growth, as measuring temperature changes to that degree of accuracy is impossible in a real body of water. In short, the mesh size did not change the results of the computation by an amount enough to be relevant to our needs, but we refined the mesh until the solution had no dependence on it.

Model Results

As seen in Figure 7, it takes a considerable amount of time for the ice freezing process to begin but once it begins after 23 days it grows quickly before slowing down as the ice sheet insulates the water below. The appearance of more than one temporary ice sheet (around 5 and 10 days) was an unexpected but reasonable result.

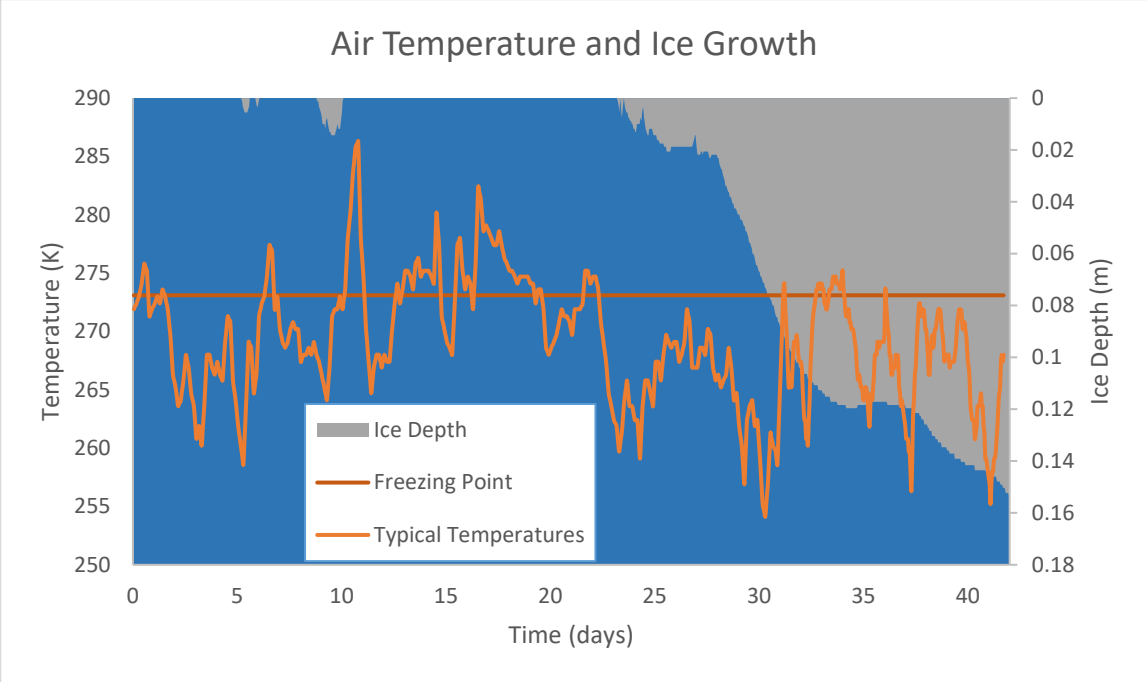

Fig. 7: Ice Freezing in Syracuse during January. This plot shows the depth of the ice sheet over time, where the initial time is midnight on January 1st.

Notice that it takes 23 days for ice to begin forming permanently, and after which the sheet grows quickly. Also notice that the ice sheet never reaches 1.13m, which is the depth required to limit photosynthesis. This means that for typical January conditions, plants are safe from not having enough light to photosynthesize.

Model Validation

Because of the ability of the model in COMSOL to easily accommodate several different environmental factors such as wind speed and ambient air temperature, we found a similar study that modeled ice sheet growth over Lake Vanajavesi in Finland [8]. This paper was also chosen for validation because it provided the source of both radiative flux equations: shortwave and longwave. We extracted the environmental data: wind speed, air temperature, and cloudiness, and ran it in our own model and obtained the results displayed below in Figure 8.

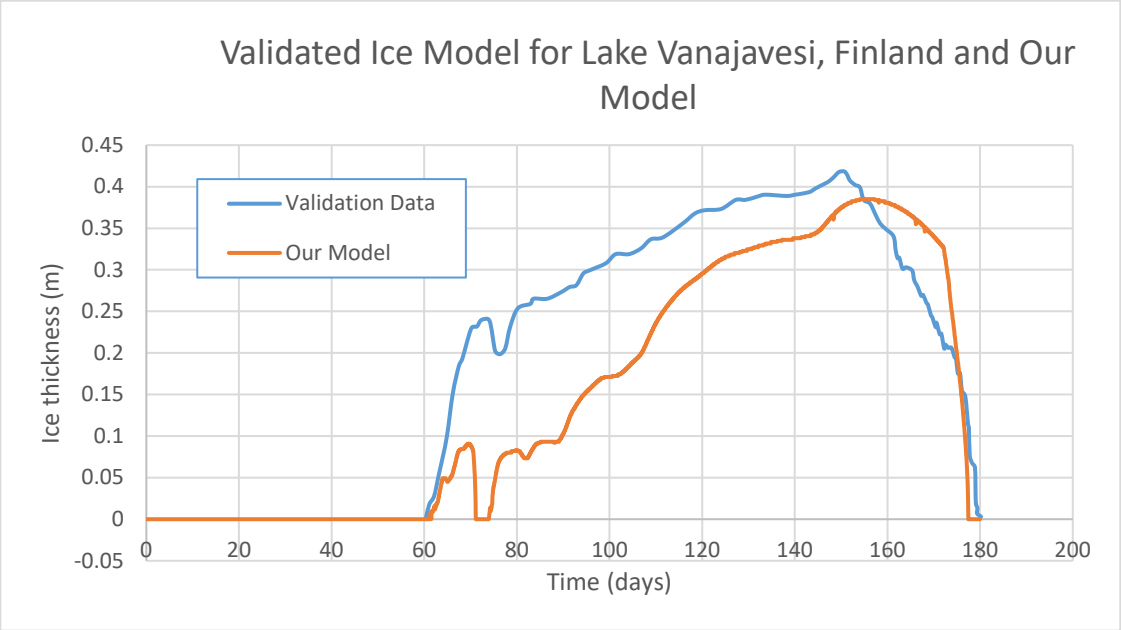

Fig. 8: Validated Ice Model of Lake Vanajavesi, Finland and Our Model. This shows the formation of the ice sheet and subsequent growth. The orange line shows our model's results for Lake Vanajavesi, while the blue line shows computational data obtained from Yang et al [8].

The two models clearly begin ice formation and have complete melting at the same time. However, during the beginning of the ice growth phase there is a difference in the growth rate of the two. Some qualitative features like the drop in depth at the beginning are similar but not exactly the same between the two models. Additionally, both models have peak ice depth occur at 155 days and at 37 cm depth.

We attribute the underestimation of depth to our snow layer. Our snow layer always exits and insulates the domain below whenever there is ice on the lake, not necessarily when snow falls from the sky and accumulates on the sheet. This approximation causes less error later in the ice sheet's life when the insulating effect of the thin snow blanket is small in comparison to the thick layer of the ice that also insulates the liquid water.

Sensitivity Analysis

We ran sensitivity analyses on the Syracuse weather conditions by varying weather conditions (Figure 9 and 11) and observed what effects this had on ice depth over time (Figure 10 and 12). We varied parameters based on reasonable variances that can be found in nature. We varied temperature by 2.8 degrees, wind speed by 10%, snow layer depth by 50%, characteristic length by 10m, cloudiness by 10%, and combinations thereof. Figure 9 (below) shows the unaltered temperature (T_{air}) and these values increased and decreased by 2.8 degrees. The model results are displayed in Figure 10.

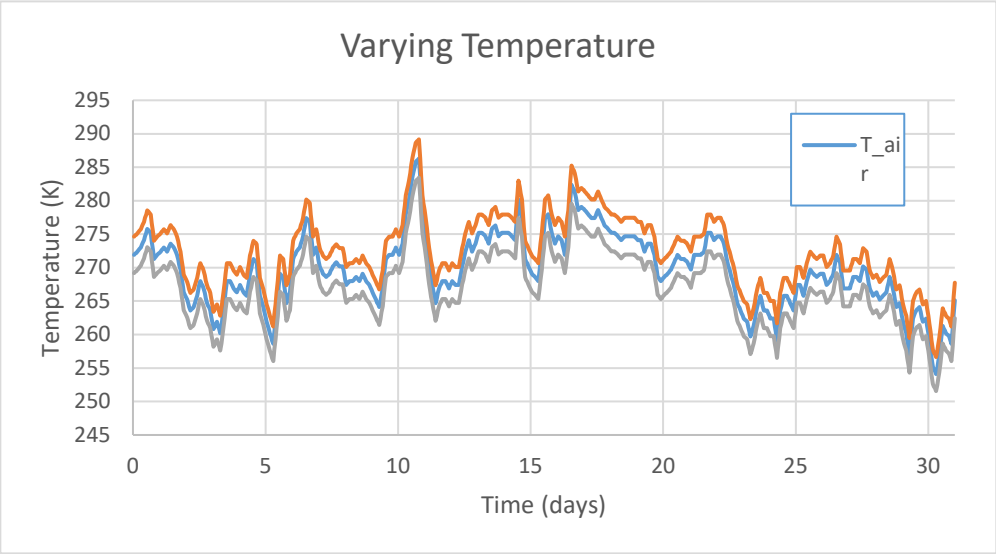

Fig. 9: Varying Temperature. This shows the temperature data from the TMY3 and that same data increased and decreased by 2.8 K. This is a large temperature change from year to year but is within reasonable physical possibility.

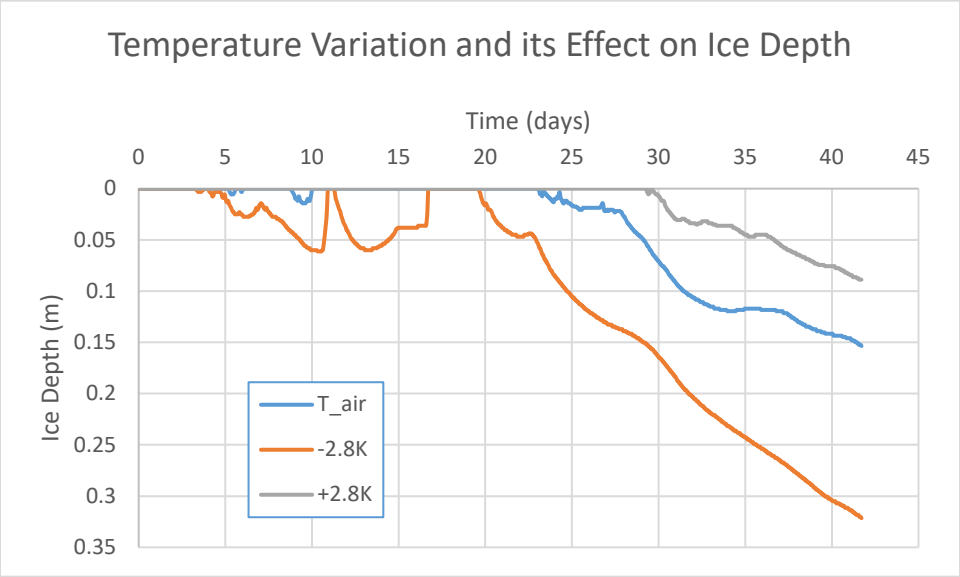

Fig. 10: Temperature Variance. This shows the effect of the changed temperature from typical weather.

Notice that changing the temperature primarily changes the formation time of the ice sheet. The curves remain parallel; the ambient temperature has less of an effect on the rate of growth. Also notice that an ice sheet forms briefly for the decreased temperature, corresponding to the cold period before warming between 3 days and 17 days. Varying temperature changes the final depth of snow more than any other parameter, indicating that temperature is the most important factor in ice sheet depth, which makes intuitive sense.

Figure 11 (below) shows the unaltered wind speed (U_{wind}) and these values increased and decreased by 10%. These model results are displayed in Figure 11.

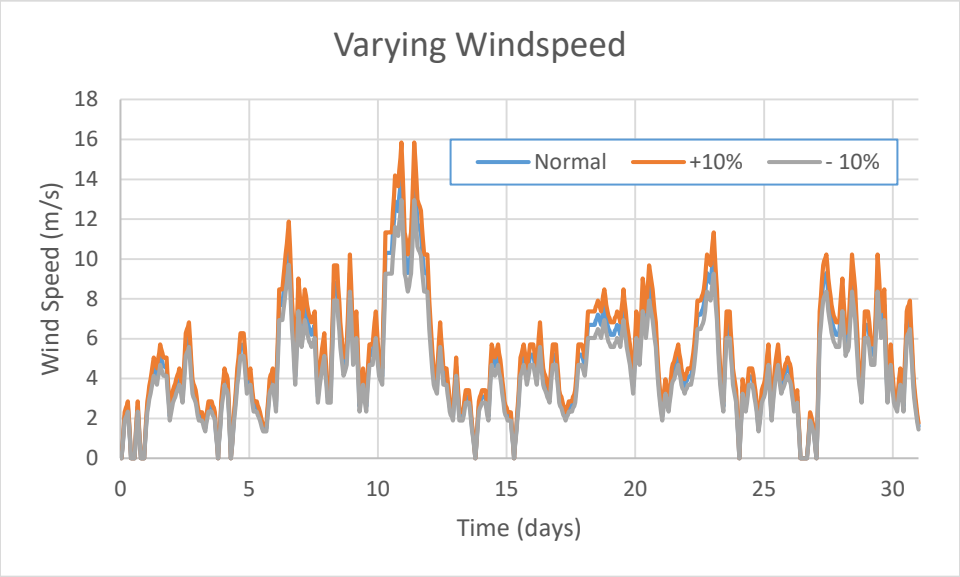

Fig. 11: Varied wind speed values. This shows the wind speed data from the TMY3 and this data increased and decreased by 10%. Given that local average wind speeds do not change drastically year to year a 10% change was deemed a reasonable amount to capture potential environmental changes.

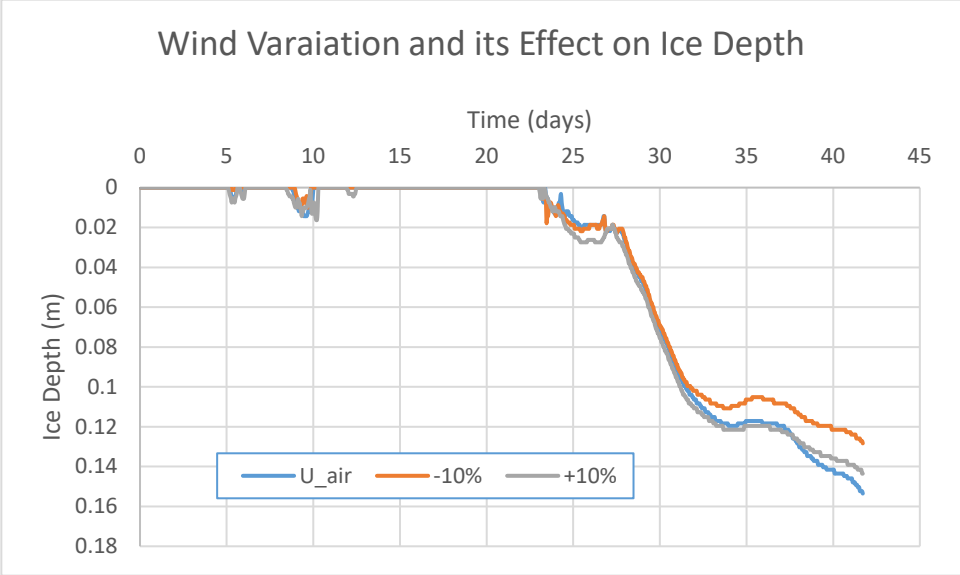

Fig. 12: Wind variance. Windiness has a relatively small effect on the ice depth in our model.

Note that unlike varying the temperature, varying the wind speed does not change the time of formation of the ice sheet. Instead, it changes the rate of growth of the ice sheet. Increasing the wind speed did not give expected results. Intuitively, we would expect that windier conditions would lead to a higher convective heat transfer coefficient and more heat loss from the lake. However we found that the windiest conditions actually lead to a more shallow ice depth than the original.

For the fetch/characteristic length we varied by 10m from the original. We varied the fetch/characteristic length more than other inputs because it can vary widely with small lakes that are often irregularly shaped. This is because a long lake could behave as if it had a characteristic length equal to either its length or width, depending on whether wind was blowing primarily along or across it, respectively. The effects of varying this length are displayed below in Figure 13.

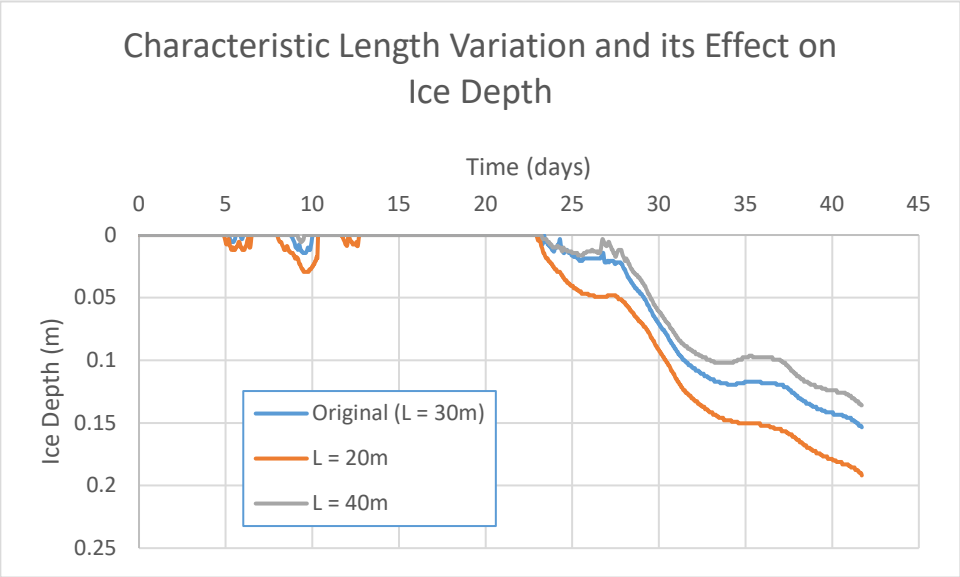

Fig. 13: Sensitivity of ice thickness to changes in characteristic length. This plot shows the dependence of the ice sheet growth on the characteristic length used in the convective heat transfer coefficient equation.

Notice that changing L has an effect on ice sheet growth rate. Decreasing the characteristic length increases the growth rate and increases ice sheet persistence (for the first, impermanent formation). This is consistent with the heat transfer coefficient equation that shows an inverse relationship between L and convective heat loss rate (h value).

Next, we examined the effects of low and high cloud conditions on ice growth. The cloudiness coefficient (CN), was varied from its original value of .80 to demonstrate the effect of increased cloud coverage with a CN of 0.90 and with a reduced CN of 0.3. The resulting differences in ice growth results are displayed below in Figure 14.

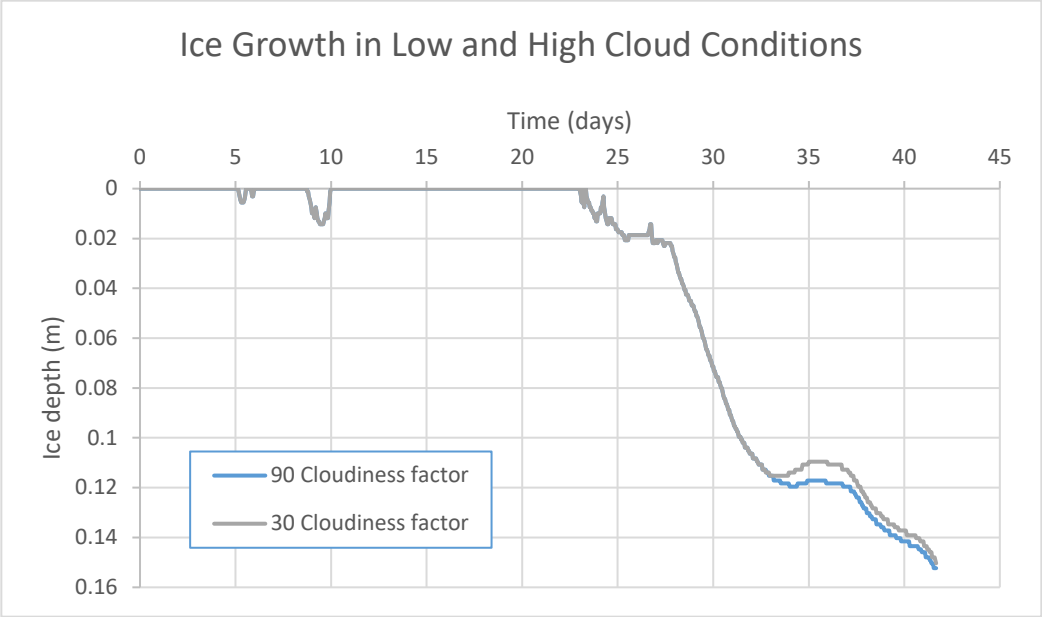

Fig. 14: Sensitivity of ice thickness to different cloud conditions in Syracuse. The normal model cloudiness coefficient is set at 0.80 for Syracuse, and was not included as it would make it nearly impossible to distinguish between the two models.

Next, we examined the effect that varying the depth of the snow layer has on ice growth. The response of the ice cover to snow layers 1 cm, 2 cm, and 4 cm thick is displayed below in Figure 15.

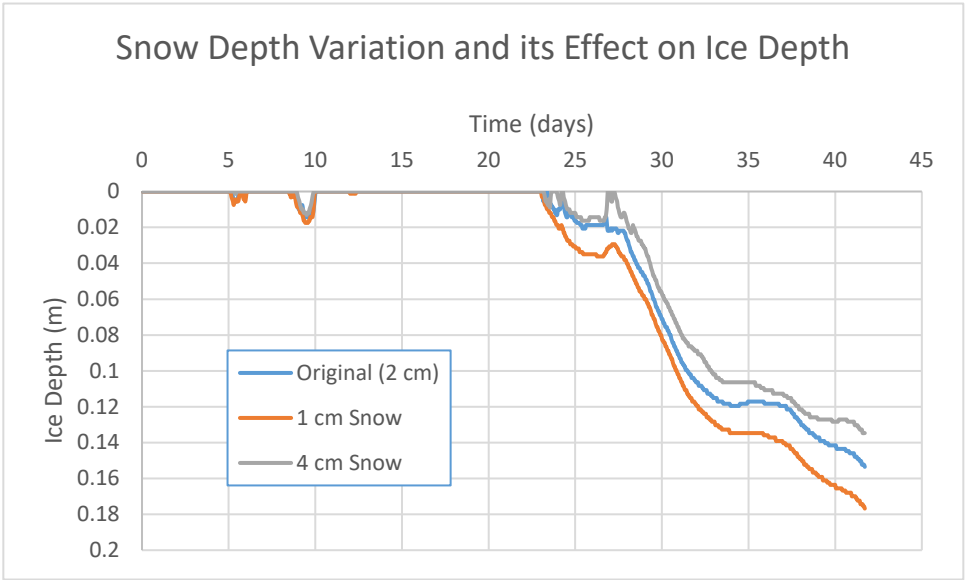

Fig. 15: Sensitivity of ice thickness to different snow cover conditions. The normal model (vanilla) included 2 cm of snow cover, and the thickness of the snow layer was varied to demonstrate the effect of varying snow cover conditions on ice formation.

Snow cover has an insulating effect that traps heat near the surface of the ice and reduces ice formation rate. This effect appears to be consistent with the results displayed in Figure 15. As the thickness of the snow layer increases, the rate of ice formation slows, and even ceases at 27 days for the thickest snow cover.

Finally, we looked at ice formation under a combination of different conditions. We compared warm, calm, and sunny conditions (quantified as a 2.8K temperature increase, 10% decrease in wind speed, and a reduced cloudiness factor of 0.72, respectively) with cold, windy, and cloudy conditions (quantified as a 2.8K temperature decrease, 10% increase in wind speed, and an increased cloudiness factor of 0.88, respectively). These results are displayed below in Figure 16.

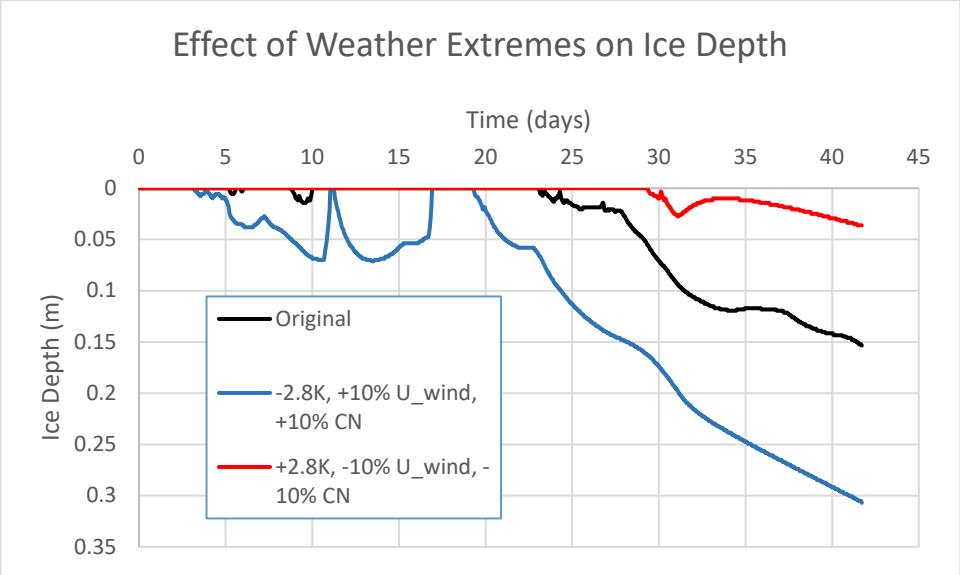

Fig. 16: Different ice thickness profiles for extreme weather scenarios. This plot shows the combined effect of temperature, wind, and cloudiness on the growth of the ice sheet. Results were consistent with expectations as well as previously conducted sensitivity analyses of individual parameters.

Sensitivity Analysis - Discussion

Based on the results from our sensitivity analysis one of the most important parameters is temperature. We expected that even small temperature changes would have a noticeable effect on when ice growth began and when it stops. Thus it is very important to use local temperature data in this model. However once local wind data and local lake measurements are made, which are relatively easy to make, our model provides an accurate estimation of local lake ice conditions. We believe this tool to be accurate enough for use in ecological studies of plants beneath the lake surface. The model is relevant outside of the Syracuse location. However, we expect at the minimum, different assumptions about the snow layer and different local Zenith angle measurements would need to be corrected if the model were to be implemented outside of this locale.

Conclusion

After examining various models of ice freezing and ice growth, we present a simple approximate model that can be used for estimating ice thickness in upstate New York or a similar Northeastern location where weather data is available. Our model incorporates time-series temperatures, wind speeds, zenith angles and cloudiness. The model accepts these inputs and uses them in convective and radiative boundary conditions to our heat conduction domain. As an output the model gives the depth of the ice sheet as a function of time. This simple set up is powerful and has a reasonable degree of accuracy with respect to other, similar studies. The discretization error was minimized through a mesh convergence, even though the error caused by discretization was small enough to not matter for the sake of this function.

We found that under typical conditions, as in the TMY3 data, lake ice formation does not reach a point deep enough to actually inhibit photosynthesis. This makes sense because underwater plants have evolved for millennia to be suited to their environment, and should be able to easily tolerate a typical winter. Our model did demonstrate this. However, even under cold, windy, and cloudy conditions that we described in our sensitivity analysis, the ice sheet was not close to being deep enough for inhibition. But, with climate change causing more and more extreme weather every winter, a future winter could be bitter enough to grow the ice sheet deep enough.

Our model performs well when looking for a simple model that can be used to run large parameter searches. However, for studies needing very high accuracy and granularity we expect our model to underperform and be unable to deliver high enough accuracy. Future modifications to improve accuracy might include accurate snowfall prediction and snow packing. However, we anticipate incorporating this into future models to be non-trivial.

Slightly different models may be needed in areas where there is a very small level of precipitation. Low precipitation would end up changing our small snow layer approximation. In locations with very little snowfall our assumption of a snow layer immediately after the ice sheet forms would be invalid and would lead to problems with our model. However, given a Northeastern US climate we are confident enough in model performance for use in large scale climate and similar studies.

Appendices

Appendix A: Input Parameters

Table 1: Parameters used in model, as well as their values (if constant) and the source they were obtained from.

Parameter	**Value**	**Source**
Surface emissivity (ε)	0.97	[9]
Average cloudiness (CN)	0.80	[10]
Air density as a function of temperature	Table 2	[11]
Boltzmann constant (σ_s)	$1.3806 \times 10^{-23}\ m^2\ kg\ s^{-2}\ K^{-1}$	[11]
Ambient air temperature (T_{air})	Displayed in Figure 4	[12]
Wind speed (U_{wind})	Displayed in Figure 4	[12]
Water density (ρ)	Displayed in Figure 3	[7]
Solar zenith angle (Z)	Displayed in Figure 17	[13]
Solar constant (S)	1366.1 W/m^2	[14]
Characteristic length	20 m	Chosen by researchers
Thermal conductivity (k)	Table 3	[15]
Water vapor pressure (vp)	Table 4	[11]

Table 2: Air density as a function of temperature

Temperature (K)	Density (kg/m^3)
258.15	1.367
263.15	1.341
268.15	1.316
273.15	1.292
278.15	1.268
283.15	1.246
288.15	1.225

Table 3: Thermal conductivity of air as a function of temperature.

Temperature (K)	Thermal conductivity (W/mK)
248.15	0.02241
258.15	0.0232
263.15	0.02359
268.15	0.02397
273.15	0.02436
278.15	0.02474
283.15	0.02512
288.15	0.0255
293.15	0.02587
298.15	0.02624

Table 4: Water vapor pressure as a function of temperature.

Temperature (K)	Water Vapor Pressure (mbar)
259.15	1.827808029
260.15	2.00105361
261.15	2.191758048
262.15	2.397235365
263.15	2.61882855
264.15	2.861909559
265.15	3.123792414
266.15	3.407163093
267.15	3.713364585
268.15	4.046425857
269.15	4.40500392
270.15	4.791784752
271.15	5.21079732
272.15	5.663384613
273.15	6.149546631

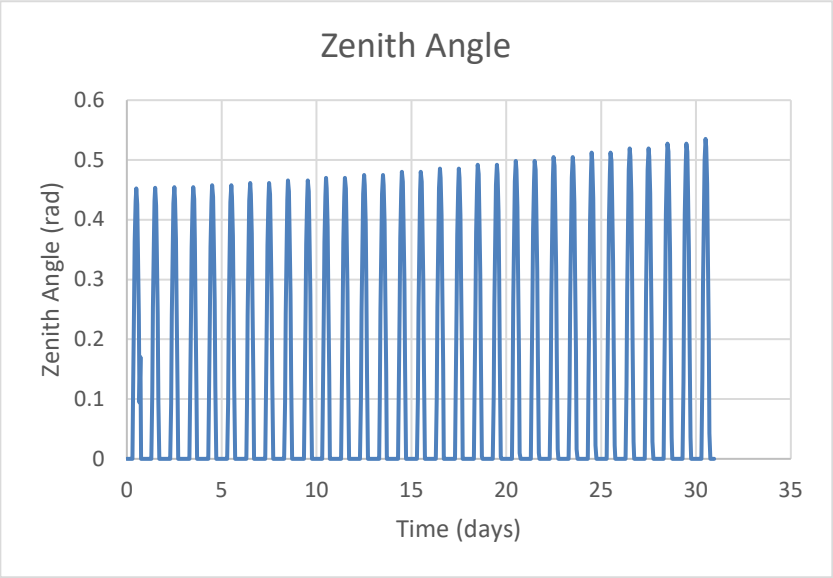

Fig. 17: Solar zenith angles in Syracuse, NY for January.

Appendix B: Numerical Implementation

The equations are solved using a commercial finite element package, COMSOL Multiphysics version 4.3b (COMSOL Multiphysics Burlington, MA). One modules in this software was used *Heat Transfer in Solids* (Eq. 1). A backward time difference discretization with an initial time step of and a maximum time step of 0.5 hours after was solved. The relative tolerance was 0.01 and absolute tolerance factor was 0.1, both tolerance methods referred to the temperature. A rectangular mesh of 2000 elements was used with maximum element width of 1.34 m and minimum element size of 0.006 m. The simulation was run using a fully coupled MultifrontalMassively Parallel Sparse direct Solver (MUMPS) this was used with an automatic non-linear solver and took 127 seconds to run on a computer with 16 gigabytes of ram with an Intel i7-6700 CPU running at 3.4 GHz. We originally had problems with the solver taking too large of a step size. This was solved by limiting the maximum time step to 0.5 hours.

Appendix C: References

Cover Photo:
"Winter Landscape Stock Vector Art 623376952." *Royalty Free Ice Lake Clip Art, Vector Images & Illustrations - IStock*, www.istockphoto.com/illustrations/ice-lake?excludenudity=true&sort=mostpopular&mediatype=illustration&phrase=ice lake.

[1] Pedersen, Ole, et al. "Underwater Photosynthesis of Submerged Plants – Recent Advances and Methods21." Frontiers in Plant Science, Frontiers Media S.A., 21 May 2013, www.ncbi.nlm.nih.gov/pmc/articles/PMC3659369/#B85.

[2] Spencer, W. E., and R. G. Wetzel. "Acclimation of Photosynthesis and Dark Respiration of a Submersed Angiosperm beneath Ice in a Temperate Lake." Plant Physiology, American Society of Plant Biologists, 1 Mar. 1993, www.plantphysiol.org/content/101/3/985.

[3] Kirk, John T. O. Light and Photosynthesis in Aquatic Ecosystems. Cambridge University Press, 2011.

[4] Duarte, Carlos M. "Seagrass Depth Limits." Aquatic Botany, no. 40, Feb. 1991, pp. 363–377., www.sciencedirect.com/science/article/pii/030437709190081F.

[5] Rolls, Robert J., Brian Hayden, and Kimmo K. Kahilainen. "Conceptualising the Interactive Effects of Climate Change and Biological Invasions on Subarctic Freshwater Fish." Ecology and Evolution 7.12 (2017): 4109–4128. PMC. Web. 27 Mar. 2018.

[6] Lepparanta, M. and Kosloff, P. 2000. The thickness and structure of Lake Pääjärvi ice. Geophysica 36, 233-248.

[7] Kell, George S. "Density, Thermal Expansivity, and Compressibility of Liquid Water from 0.Deg. to 150.Deg.. Correlations and Tables for Atmospheric Pressure and Saturation Reviewed and Expressed on 1968 Temperature Scale." *Journal of Chemical & Engineering Data*, vol. 20, no. 1, 1975, pp. 97–105., doi:10.1021/je60064a005.

[8] Yang, Yu, et al. "Numerical Modelling of Snow and Ice Thicknesses in Lake Vanajavesi, Finland." *Tellus A: Dynamic Meteorology and Oceanography*, vol. 64, no. 1, Feb. 2012, p. 17202., doi:10.3402/tellusa.v64i0.17202.

[9] Vihma, T. 1995. Subgrid parameterization of surface heat and momentum fluxes over polar oceans. J. Geophys. Res. 100, 22625-22646.

[10] Drebs, A., Nordlund, A., Karlsson, P., Helminen, J. and Rissanen, P. 2002. Climatological Statistics of Finland 1971-2000. Finnish Meteorological Institute, Helsinki.

[11] Perry, Robert H., et al. Perry's Chemical E*ngineers' Handbook*. McGraw-Hill, 1997.

[12] NSRDB update - TMY3: Alphabetical List by State and City. (n.d.). Retrieved from http://rredc.nrel.gov/solar/old_data/nsrdb/1991-2005/tmy3/by_state_and_city.html#S

[13] NOAA Solar Position Calculator. (n.d.). Retrieved from https://www.esrl.noaa.gov/gmd/grad/solcalc/azel.html

[14] Yang, Dazhi, et al. “Estimation and Applications of Clear Sky Global Horizontal Irradiance at the Equator.” *Journal of Solar Energy Engineering*, vol. 136, no. 3, Feb. 2014, p. 034505., doi:10.1115/1.4027263.

[15] Rashid, T., Khawaja, H., & Edvardsen, K. (2016). Determination of Thermal Properties of Fresh Water and Sea Water Ice using Multiphysics Analysis. *The International Journal of Multiphysics,10*(3), 277-292. doi:10.21152/1750-9548.10.3.277